Deliverable D6 (D1.6)

Observational methodologies for horizontal & vertical profiling for AQ purposes

RI-URBANS

Research Infrastructures Services Reinforcing Air Quality Monitoring Capacities in European Urban & Industrial AreaS (GA n. 101036245)

By

CNRS, CNR, INOE, FZJ & KNMI

29th September 2022

RI-URBANS (www.RIURBANS.eu) is supported by the European Commission under the Horizon 2020 – Research and Innovation Framework Programme, H2020-GD-2020, Grant Agreement number: 101036245

Deliverable D6 (D1.6): Observational methodologies for horizontal & vertical profiling for AQ purposes

Authors: Martial Haeffelin (CNRS), Simone Kotthaus (CNRS), Lucia Mona (CNR), Francesca Barnaba (CNR), Anna Chiara Bellini (CNR), Doina Nicolae (INOE), Andreas Petzold (FZJ), Christoph Mahnke (FZJ), Arnoud Apituley (KNMI)

Work package (WP)	WP1 T1.3 Developing products and methods for AQ from profiling observations
Deliverable	D6 (D1.6)
Lead beneficiary	CNRS
Deliverable type	■ R (document, report) ☐ DEC (websites, patent filings, videos,….) ☐ Other: ORDP (open research data pilot)
Dissemination level	■ PU (public) ☐ CO (confidential, only members of consortium and European Commission))
Estimated delivery deadline	30/09/2022
Actual delivery deadline	29/09/2022
Version	Final
Reviewed by	WP1 Leaders and Coordination Team
Accepted by	RI-URBANS Project Coordination Team
Comments	This document provides information about several atmospheric products (atmospheric boundary layer height, aerosol profiles, reactive trace gas profiles, wind and turbulence profiles) that can efficiently complement 'standard' in situ air quality data for different applications, including assessment, monitoring, and forecast. The document also presents a few selected examples of measurements and retrievals that are currently in operation in some European cities and finally outlines the instrument requirements necessary to retrieve the products presented.

RI-URBANS (www.RIURBANS.eu) is supported by the European Commission under the Horizon 2020 – Research and Innovation Framework Programme, H2020-GD-2020, Grant Agreement number: 101036245

Table of Contents

RI-URBANS (www.RIURBANS.eu) is supported by the European Commission under the Horizon 2020 – Research and Innovation Framework Programme, H2020-GD-2020, Grant Agreement number: 101036245

1 About this document

Currently most Air Quality Monitoring Networks (AQMNs) miss information about important processes and quantities along the vertical dimension that are necessary to better understand surface-level pollution data. This is relevant to take into account potential non-local sources of aerosols (e.g. those from medium-to-long-range transport) but also to evaluate vertical dilution of locally emitted pollutants and, in specific conditions, episodes associated with new particle formation and related particle growth processes.

This document provides information about several atmospheric products (atmospheric boundary layer height, aerosol profiles, reactive trace gas profiles, wind and turbulence profiles ; Section 2: Products) that can efficiently complement 'standard' in situ Air Quality (AQ) data for different applications, including assessment, monitoring, and forecast. The document also presents a few selected examples of measurements and retrievals that are currently in operation in some European cities (see Section 3: *Showcase*) and finally outlines the instrument requirements necessary to retrieve the products presented (Section 4: *Measurement requirements*).

This deliverable addresses Task 1.3 on developing products and methods for AQ from profiling observations. This task develops Service Tools (STs) for observations with vertical and/or horizontal scanning capability in and around urban environments from ACTRIS and IAGOS. Measurement requirements are being provided for the implementation in the pilots, observational and procedural methodologies for the use of these data for urban AQ purposes.

This is a public document, available in the RI-URBANS website (https://riurbans.eu/work-package-1/#deliverables-wp1). The document will be distributed to all RI-URBANS partners for their use and submitted to European Commission as an RI-URBANS delieverable D6 (D1.6).

2 Products

2.1 Atmospheric Boundary Layer Height

The Atmospheric Boundary Layer (ABL) height indicates the height of the atmospheric layer that is directly affected by surface-atmosphere exchanges. It includes the height of the mixed layer (MLH) and the height of the residual layer (RLH) at night, which are both relevant for AQ. The MLH defines the volume of air in which atmospheric constituents emitted at the Surface (or also some altitude within the ABL) get mixed and diluted. In the residual layer, formation of secondary aerosols can be significant, that are then entrained into the mixed layer during morning growth. The MLH and RLH can be derived from different atmospheric profile observations, using thermodynamic (based on temperature/humidity), dynamic (based on wind or turbulence variables), trace gas-based (e.g. ozone) or aerosol-based approaches, or some synergy of those methods, respectively. A recent review paper by Kotthaus et al. (2022) presents the different methods available and their capabilities and limitations depending on atmospheric conditions and measurement setup. Algorithms for the retrieval of layer heights from profile observations are becoming increasingly advanced, now often including checks for temporal consistency or automatic quality control procedures.

For RI-URBANS two advanced processing algorithms are being implemented that derive MLH (and RLH) from automatic lidar and ceilometer (ALC) observations (Section 4.2) using tailored aerosol-based retrieval approaches:

RI-URBANS (www.RIURBANS.eu) is supported by the European Commission under the Horizon 2020 – Research and Innovation Framework Programme, H2020-GD-2020, Grant Agreement number: 101036245

the STRATfinder and the CABAM algorithm, applied to data collected by ALC with a relatively high and low signal strength, respectively (Kotthaus et al. 2020).

MLH products are currently derived in near real-time for the following Pilot cities: Paris (5 sites), Bucharest (2 sites), Helsinki (2 sites), Rotterdam (rural site Cabauw), and Aosta (affected by Milan). Quicklooks are accessible here:

- Paris region network: https://observations.ipsl.fr/aeris/ABLH-paris/
- European network: https://observations.ipsl.fr/aeris/e-profile/

In addition, the italian ALC network ALICEnet is implementing the MLH detection using STRATfinder at measurement sites in Milan and Rome.

Another MLH retrieval method exploiting attenuated backscatter signals using artificial intelligence (AI; Vivone et al., 2021) could be tested in the framework of RI-URBANS for selected sites (e.g. Milan) provided suitable measurement conditions as this method was found promising for intensive application to aerosol lidar and ALC measurements.

2.2 Aerosol optical property profiles

Aerosol optical property profiles provide insights on the vertical distribution of the aerosols, their dynamics in time and vertical dimensions. These characteristics are important for Air Quality issues because some lofted layers can intrude in the ABL thereby impacting near-surface AQ. Additionally, the use of aerosol optical properties jointly with model simulations can improve forecasts through assimilation and their assessment through evaluation. Over Europe the EARLINET (European Aerosol Research LIDar NETwork) is providing high quality aerosol optical properties vertical profiles since 2000. Now EARLINET is part of ACTRIS (Aerosol Clouds Trace Gases Research InfraStructure) as its aerosol remote sensing component. During this path toward the ACTRIS research Infrastructure, EARLINET worked on the harmonisation of measurements collection, data provision and data processing (Pappalardo et al., 2014). In particular, a centralised processing system able to process the data from raw data to quality control vertical profiles of multiwavelength aerosol extinction and backscatter coefficients and volume and particle depolarization profiles from lidar elastic and Raman backscattering profiles has been developed and is available for all the lidar stations (D'Amico et al., 2015, D'Amico et al., 2016, Mattis et al., 2016). Measurements are not performed continuously as the systems are not always operated fully automatically and autonomous and those observations are rather costly. Data analysis is typically done at station level with a certain timeliness (typically data are provided after 1 year from the measurements). However, a pilot provision of data in NRT to CAMS (Copernicus Atmospheric Measurement System) proved the current capability of EARLINET/ACTRIS of providing aerosol optical property profiles in near real time at continental scale (Mona et al., EGU2021). Four EARLINET/ACTRIS stations located in (or near) RI-URBANS pilot cities have set up all the features for NRT provision to CAMS:

- Bucharest,
- Palaiseau,
- Barcelona and
- Warsaw.

The possibilities of identifying layers and their characteristics based on the aerosol optical property profiles of extinction and backscatter are widely demonstrated in the literature. One example of a volcanic aerosol layer travelling long distances before being entrained into the ABL, eventually reaching the surface is presented by Mona et al. (2012). The plume emitted in Iceland in 2010 reached Southern Italy after a long-distance travel across Europe: multiwavelength Raman observations allowed for the layer identification, the investigation of its temporal behaviour in terms of affected altitude and in terms of particles characteristics (lidar ratio, depolarization).

RI-URBANS (www.RIURBANS.eu) is supported by the European Commission under the Horizon 2020 – Research and Innovation Framework Programme, H2020-GD-2020, Grant Agreement number: 101036245

2.3 Aerosol type profiles

The aerosol type profile is defined as a vertical sequence of aerosol classes (such as continental, continental polluted, smoke, dust, volcanic, marine) that dominate within the aerosol layers present at a certain location in the troposphere. In some cases, even mixtures of multiple aerosol types in a given layer can be characterised. Aerosol type profiles are of interest for AQ because the long-range transport of aerosols may affect the local AQ at the ground after entrainment into the ABL (or indirectly through potential alterations of the atmospheric radiation budget). Such aerosol classification exploits the contrasting optical characteristics associated with the various aerosol types. For example, dust and volcanic particles have a high depolarization, smoke from fires is highly absorbant, while marine aerosols tend to be spherical and not absorbing. Different approaches and methods (e.g. decision trees, multispace attribution, neural network) have been developed for aerosol type classification. Comparison studies reveal the respective capabilities and limitations of such methods (Nicolae et al., 2018; Papagiannopoulos et al., 2018; Voudouri et al., 2019). Often, aerosol type profiles are determined based on observations from multi-wavelength depolarization Raman aerosol lidars. A particular example of the aerosol type identification is showcased for an event in Bucharest (Section 3.2). But also polarization-sensitive ALC (P-ALC), capable of monitoring the particle depolatisation profile continuously, are becoming available. Selected case studies are presented to demonstrate the application of such data for aerosol typing in Aosta, Milan and Paris (Section 3.3).

Aerosol type profiling from Raman Lidars will be implemented in the follow pilot cities:

- Bucharest,
- Palaiseau,
- Barcelona and
- Warsaw

Aerosol type profiling from P-ALC is not planned to be implemented in RI-URBANS pilot cities.

2.4 Aerosol mass concentration profiles

Aerosol mass concentration profiles are of interest for air quality because they can complement the particulate matter mass concentrations (PM) measured routinely at the ground by AQMN as requested by the European AQ Directive 2008/50. The vertical profile of aerosol mass concentration is also important for direct comparison with standard outputs of AQ numerical models and for their possible improvement, as these provide an observation-based insight of the processes affecting 3D fields of PM, and thus AQ. In fact, as mentioned above, the lower atmosphere is a highly dynamical environment, and PM measurements at the ground can be strongly affected by the vertical and horizontal motion of atmospheric layers at different spatial and temporal scales.

There are different algorithms for retrieving information about PM concentration profiles. Müller et al. (2019) and Veselovskii et al. (2012) describe the use of multiwavelength + depolarization lidar measurements, as stand-alone aerosol concentration profile retrievals with low (below 20%) statistical errors and high constraints.

More automatic and relatively easier methods to be applied in a systematic and autonomous way make use of combined lidar and co-located photometer measurements for getting columnar integrated information about concentration. Based on these requirements ACTRIS aerosol remote sensing component requires for each measurement site the lidar and photometer collocation, and is developing a combined data product. At the time being, the GARRLiC (Generalized Aerosol Retrieval from Radiometer and Lidar Combined data) algorithm (Lopatin et al., 2013) is working experimentally on EARLINET data and collocated simultaneous AERONET data for retrieving

RI-URBANS (www.RIURBANS.eu) is supported by the European Commission under the Horizon 2020 – Research and Innovation Framework Programme, H2020-GD-2020, Grant Agreement number: 101036245

interesting parameters. Figure 1 shows an example of concentration profiles determined by GARRLiC over Finokalia in Crete: volume concentration and its fine and coarse components are reported. In this case, the coarse particles are associated with marine aerosols while the fine contribution is from local pollution (Tsekeri et al., 2017). GARLLiC performs well, when compared to another lidar inversion algorithm (i.e. LIRIC, LIdar-Radiometer Inversion Code; Chaikovsky et al., 2016) and also to in-situ observations or model results (Tsekeri et al., 2017).

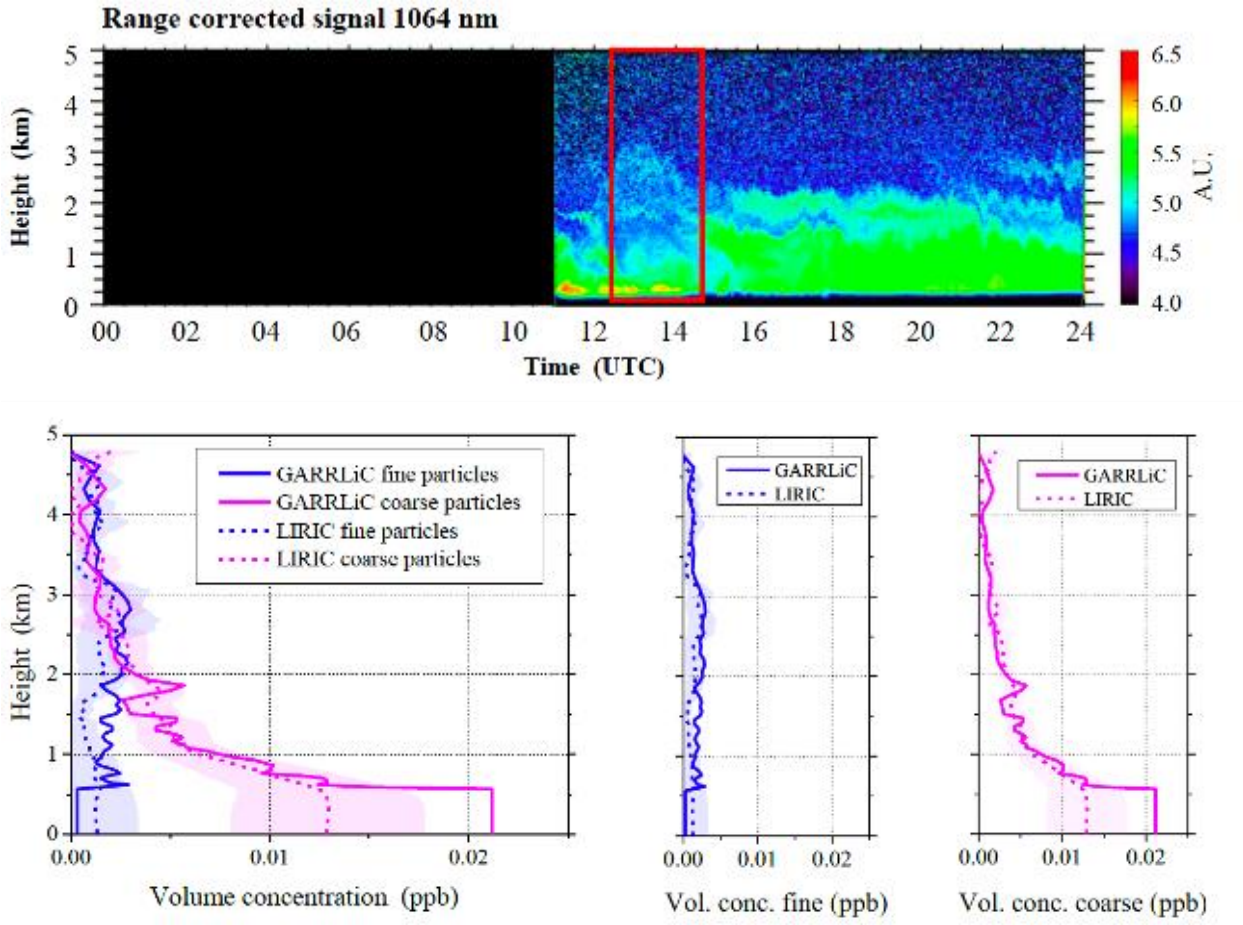

Figure 1 *: Example of aerosol volume concentration profiles from aerosol lidar measurements performed at Finokalia, Crete on 15 July 2014, at 12:30–14:30 UTC. Temporal evolution of range corrected lidar signal on top and retrieved concentration profiles for the red box time interval in the bottom part of the plot. Two algorithms are here showed GARRLiC and LIRIC. The figure is an elaboration of figures 7 and 10 of Tsekeri et al. (2017).*

For the advanced multiwavelength Raman lidars located at background and reference locations close to the RI-URBANS Pilot cities, GARRLIC products can be provided. These products have been evaluated in the framework of various campaigns and the observations and are sufficiently mature to commence implementation in the automatic ACTRIS processing chain.

In addition to the highly accurate observations of aerosol mass concentration profiles using research lidars, this product can also be derived from ALC profile observations. Compared to Raman lidars, logistics are minimal as these simple, affordable, compact lidar systems operate automatically and continuously with eye-safe lasers and very low maintenance. They hence provide valuable monitoring capabilites for AQ applications. Such low-cost, low-maintenance instruments can be directly integrated into AQMN infrastructures, allowing for aerosol mass

RI-URBANS (www.RIURBANS.eu) is supported by the European Commission under the Horizon 2020 – Research and Innovation Framework Programme, H2020-GD-2020, Grant Agreement number: 101036245

concentration profiles to be retrieved directly at the AQMN sites (as, e.g., within the Italian ALICEnet network). Data processing to derive aerosol mass concentration profiles from ALC raw data needs some caution and expertise, but promising examples of centralised data processing for operational purposes are ongoing (e.g., by ALICEnet, Met Office, EUMETNET E-PROFILE).

Despite the greater uncertainty compared to research lidar products, this operational (24/7) product is already proving to be extremely useful for the interpretation of the local and non-local phenomena that influence the PM data collected at the ground by AQMN (e.g. Diemoz et al., 2019a, 2019b). It can also represent a common base of comparison with AQ models, typically providing PM fields simulations. This product will be tested in the project against high-performance lidar and/or high-performance lidar plus photometer products.

As an example of ALC-based, PM information, Figure 2 shows a multi-annual (6-year) climatology of PM10 vertical profiles derived within the RI-URBANS WP1 activities at two major suburban ALICEnet sites in Italy (the RI URBANS Pilot city Milan, and Rome). The ALICEnet PM10 retrieval has been evaluated using long-term datasets and measurement campaigns (e.g. Bellini et al., 2022). Additional examples of ALC-based PM retrieval results and comparisons to models are provided in Section 3.4 focusing on the Po Valley RI-URBANS Target Region region.

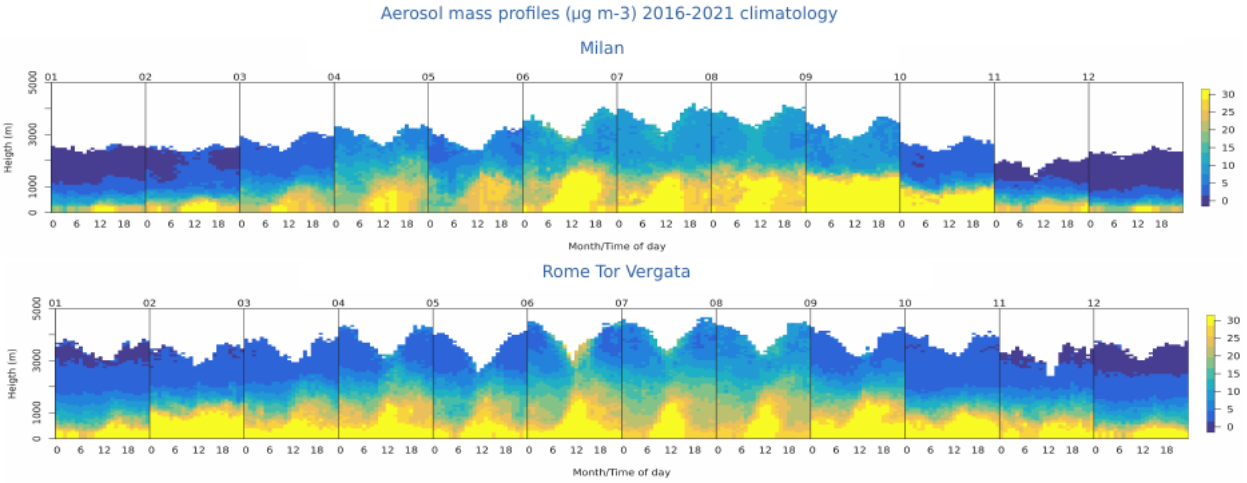

***Figure 2** : Multi-annual (2016-2021) climatology of the monthly-(top axis month of the year) and daily-(bottom axis hour of the day) resolved profiles of the aerosol mass (µg/m3) as derived from the ALICEnet systems in the two suburban areas of Milan and Rome (Bellini et al., 2022).*

Aerosol mass concentration profiling from Raman Lidars will be implemented in the follow pilot cities:

- Bucharest,
- Palaiseau,
- Barcelona, and
- Warsaw

Aerosol mass concentration profiling from ALC will be implemented in the follow pilot cities:

- Milan,
- Paris (TBC)

RI-URBANS (www.RIURBANS.eu) is supported by the European Commission under the Horizon 2020 – Research and Innovation Framework Programme, H2020-GD-2020, Grant Agreement number: 101036245

2.5 Gas concentration profiles

Using in-situ sensors carried by passanger air planes, the In-service Aircraft for a Global Observing System1 (IAGOS) monitors vertical profiles of trace gas concentrations (incl. CO, O3, NO2 and NOx) near airports during take-off and landing. These profiles characterise the vertical distribution of trace gases in the background atmosphere that interacts with the urban boundary layer. In addition, elevated layers that are often advected via regional or long-range transport are assessed with respect to their pollution concentrations. These data provide valuable information that is complementary to the surface-based AQMN stations, facilitating the link to high-resolution models and satellite observations. Trace gas measurements by the IAGOS network have different levels of maturity (Table 1).

Table 1: *Trace gas measurements by the IAGOS.*

Trace gas	Measurement approach	Reference	Level of maturity
CO	Infrared absorption using the gas filter correlation technique	Nédélec et al. (2015)	high maturity
O_3	UV absorption at 253.7 nm	Nédélec et al. (2015)	high maturity
NO_2	Cavity Attenuated Phase Shift (CAPS) provides a direct absorption measurement	Kebabian et al. (2008)	to be tested
NO_x	chemiluminescence (NO and NO_x sequentially, by switching the LEDs of the photolytic converter off and on)	Berkes et al. (2018)	mature

2.6 Vertical profiles of wind and turbulence

Aerosol and trace gas spatial distributions (horizontal and vertical) are significantly affected by both the mean wind field (wind speed and direction) as well as turbulent processes. This dynamics in the ABL can be observed continuously at high temporal and vertical resolution using ground-based Doppler Lidars. Doppler Lidars can be operated in different scanning modes to monitor different variables : vertical profiles of horizontal wind speed and wind direction, and vertical wind speed are retrieved in Doppler beam swinging mode (DBS) or velocity azimuth display (VAD) mode (see e.g., Liu et al. 2019). Different turbulent variables (vertical velocity variance, eddy dissipation rate) can be derived from vertical stare sampling at high temporal resolution.

Vertical profiles of wind and turbulence will be implemented in the following pilot cities :

- Paris,
- Warsaw
- Rotterdam
- Helsinki (TBC)
- Bucarest (TBC)

[1] https://www.iagos.org/

RI-URBANS (www.RIURBANS.eu) is supported by the European Commission under the Horizon 2020 – Research and Innovation Framework Programme, H2020-GD-2020, Grant Agreement number: 101036245

3 Showcases

The described advanced products derived from ground-based profile remote sensing or operational in-situ airborne observations (Section 2) provide valuable insights that can support local AQMN activities. Information in the vertical dimension helps to understand effects of medium-to-long-range transport, vertical mixing, dilution, or entrainment processes. Where observations are collected across sensor networks, also horizontal variations can be detected that can reveal certain atmospheric flow and advection mechanisms. The following examples showcase how the proposed products help to understand spatio-temporal variations in ABL aerosol and gas distributions. Automatically-derived ABL height reveals clear temporal and spatial patterns (Section 3.1). High-quality profiles of aerosol optical properties and aerosol type can be derived from multi-wavelength research lidars for specific cases (Section 3.2). Depolarisation profiles from P-ALC observations enable aerosol typing more continuously (Section 3.3). Both types of instruments can be used to derive valuable products for the characterisation of different processes that influence the ABL composition, including e.g. entrainment of aerosol from aloft after long-range transport or horizontal advection via regional-scale transport mechanismns. Section 3.4 presents how ALC profile measurements are used to quantify the impact of regional air circulation on PM-related AQ in the Po Valley and surrounding areas. These transport processes are important when it comes to planning decisions aiming to improve air quality but also in the context of AQ monitoring and reporting. In fact, the EU directive allows for subtraction of aerosol contributions brought to the region via long-range transport in the context of threshold exceedance levels. Trace gas profiles obtained from operational in-situ observation on board of passenger airplanes (IAGOS) enable the assessment of the atmospheric urban background (Section 3.5). Wind and turbulence profiles observed with Doppler wind lidars provide direct measures of average flow and mixing processes (Section 3.6).

3.1 ABL height variability (temporal & spatial)

MLH is derived operationally at multiple locations in or near selected RI-URBANS Pilot cities (Section 2.1). The long-term MLH observations allow for the variability of ABL dynamics to be evaluated at different temporal scales.

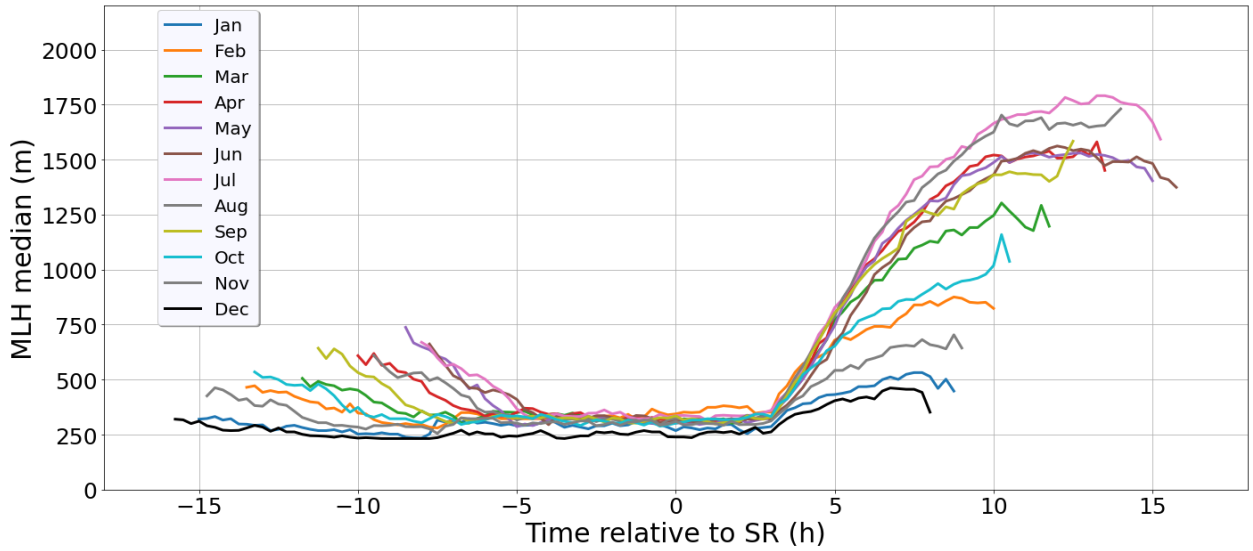

Figure 3 *: Monthly median mixed layer height (MLH) against time relative to sunrise (SR) derived from ALC profile observations (Lufft CHM15k) using the STRATfinder algorithm at the Palaiseau/SIRTA site near Paris, France, for 2015-2021.*

For example, monthly median diurnal MLH at the Palaiseau/SIRTA site near Paris derived from a 6-year dataset (Figure 3) reveal vertical buoyancy commences three hours after sunrise (SR) independently of the season. Day-to-

RI-URBANS (www.RIURBANS.eu) is supported by the European Commission under the Horizon 2020 – Research and Innovation Framework Programme, H2020-GD-2020, Grant Agreement number: 101036245

day variations can be significant. The mixed layer decays on average several hours after sunset. As expected, month-to-month variations are detected with peak daytime developments in July and August and most shallow layer heights in December and January. Note that median MLH developments are quite similar in April, May, June and September, in spite of large differences in daylight duration and peak solar elevation. Similar analyses are being performed for other locations in or near RI-URBANS pilot cities (Paris, Bucharest, Helsinki, Rotterdam/Cabauw, Aosta/Milan, and Rome). Such information is highly relevant for AQ assessments and pollution mitigation strategies in the Pilot cities, but also at regional scale (e.g., Po Basin or even the European Mediterranean area).

MLH varies spatially across an urban area. Comparisons (Figure 4) between the sub-urban site at Palaiseau/SIRTA and the central urban site at Paris/QUALAIR-SU reveal that the MLH can often reach higher levels at the urban site during daytime by several tens to hundreds of meters. Where urban ALC measurement networks are set up with sufficient density to capture the rural–suburban–urban transect, such spatial variations can be detected and quantified with the automatic procedures implemented by RI-URBANS. A dense ALC measurement network is also valuable to assess the implications of topography on the development of the layer heights.

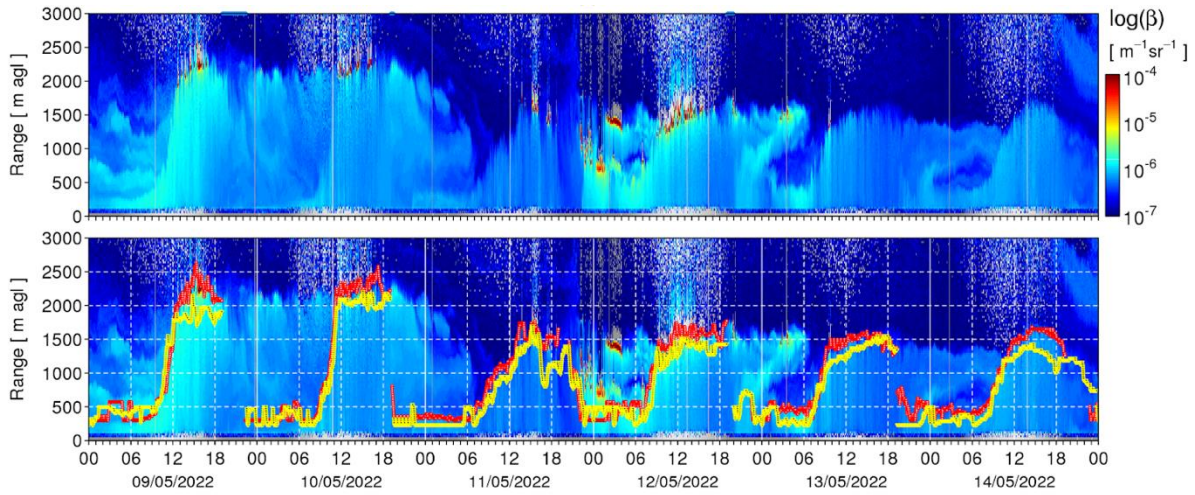

Figure 4 : *Attenuated backscatter profiles observed with an ALC (Lufft CHM15k) at the central Paris site of QUALAIR-SU between 9-15 May 2022. The bottom figure shows also the STRATfinder-derived MLH at Paris/QUALAIR-SU (campus of Sorbonne Université - red curve) in the city centre and the suburban site of Palaiseau/SIRTA (Campus of Ecole polytechnique, yellow curve), located 20 km SW from the Paris city centre.*

3.2 Aerosol typing and optical properties profiling: examples at Bucharest

Temporal series of aerosol type profiles can help identify (i) the presence of aerosol layers with particles of non-local origin and (ii) their intrusion into the ABL. An example is the detection of explosions-related smoke particles travelling from Ukraine to Romania between 14-23 of March 2022. The meteorological context favoured the transport of air masses from Ukraine towards MARS (Magurele centre for Atmosphere and Radiation Studies), an atmospheric observatory located 8 km South-West Bucharest city. Lidars and ALC operate here on routine basis. They detected the smoke particles generated by the explosions arriving at MARS at low altitudes. A first estimation of the aerosol source is possible based on the altitude of the layer (measured both by lidar and ALC) and a Lagrangean transport model (e.g. FLEXPART or HYSPLIT). The aerosol type as a function of altitude is then retrieved based on the multiwavelength capabilities of the lidar (Figure 5). In the afternoon of the 19th March 2022, the ABL reached a height of about 2 km and was composed mainly of spherical particles. In addition, two lofted layers of

RI-URBANS (www.RIURBANS.eu) is supported by the European Commission under the Horizon 2020 – Research and Innovation Framework Programme, H2020-GD-2020, Grant Agreement number: 101036245

different origins were observed: the lower layer composed of spherical particles while the upper layer also contained non-spherical particles.

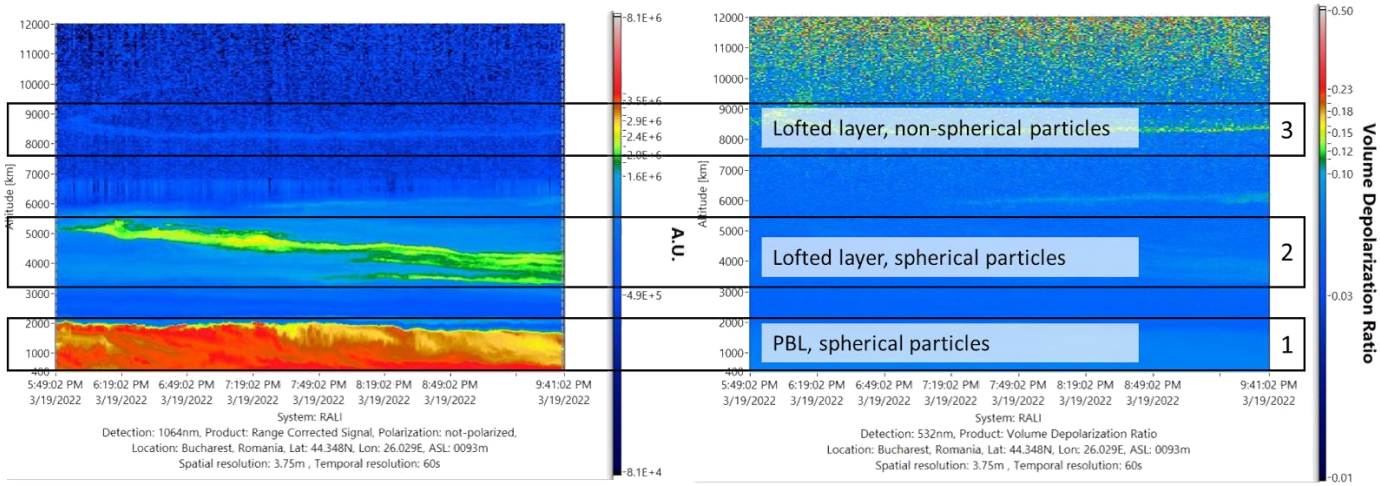

Figure 5 : *Range Corrected Signal for the 532 nm aerosol lidar elastic cross channel (left panel) and the Volume Depolarization Ratio at the same wavelength (right panel) measured at MARS on 19 March 2022, 17:49 – 21:41 UTC.*

The backward trajectory model HYSPLIT (Stein et al., 2015) shows that the air masses arriving at both 0.5 km and 4.0 km altitude may have been carrying particles from East Ukraine (Figure 6). For the latter, some of the paths were crossing the Black Sea. At 8.5 km again, the air had travelled at high altitudes for more than 72 h and therefore their origin cannot be estimated.

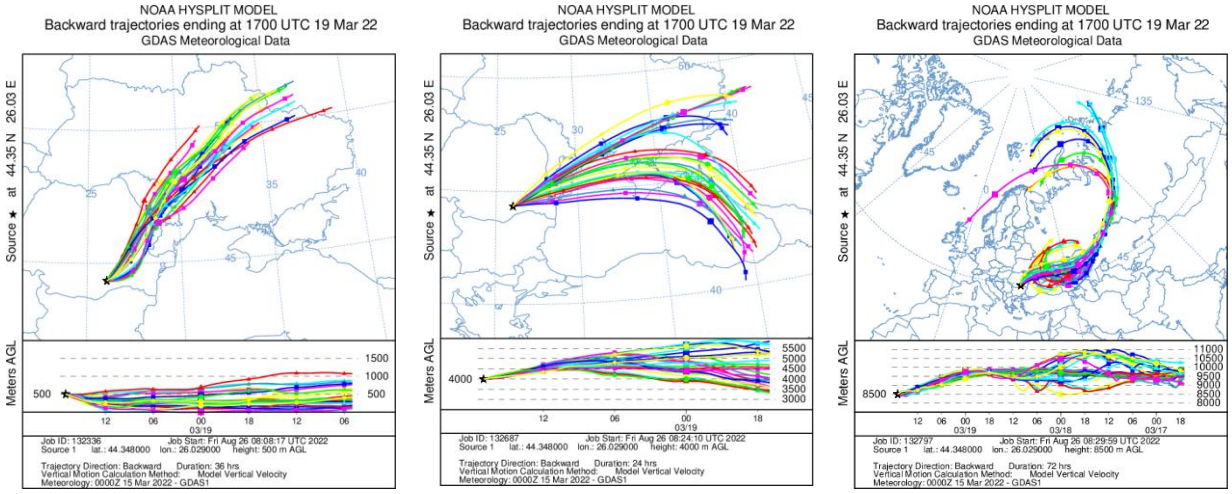

Figure 6 *: HYSPLIT ensemble back-trajectories for the particles arriving at MARS on 19 March 2022, 17:49 – 21:41 UTC at: a) 0.5 km altitude (left panel, 24 h back); b) 4.0 km altitude (middle panel, 24 h back); c) 8.5 km altitude (right panel, 72 h back).*

The profiles of optical properties measured by the lidar can help to further characterise the two aerosol layers below 6pm. The layers show a behaviour typical of smoke particles (medium to large spectral difference at the 3 wavelengths, low depolarization), only the rather low values of the lidar ratios are a bit unusual (Figure 7). The observations are consistent with the estimation of the aerosol type and source by the FLEXPART model (Pisso et al., 2019; Figure 8) as well as the results obtained from the neural network aerosol-typing algorithm based on lidar data NATALI (Nicolae et al., 2018; Figure 9). The latter allows the automatic estimation of the aerosol type from

RI-URBANS (www.RIURBANS.eu) is supported by the European Commission under the Horizon 2020 – Research and Innovation Framework Programme, H2020-GD-2020, Grant Agreement number: 101036245

multiwavelength lidar observations (3 aerosol backscatter coefficients and 2 extinction coefficients) based on the simultaneous analysis of layer-intensive optical parameters (Angstrom exponents, color ratios, lidar ratios and particle depolarization). As Figure 9 covers the period 19-28 March 2022, it should be noted that after the cloudy weather on 22nd and 23rd March, the transport changed, air masses coming predominantly from West and North Europe. Dust particles were detected in the free troposphere in addition to clean continental and continental polluted.

Multiwavelength Raman + depolarization lidars can provide a solid aerosol typing classification. For the aim of RI-URBANS, background conditions can be provided by long-term performing EARLINET measurement sites (like Cabauw, Palaiseau, Ispra and Bucharest-Magurele).

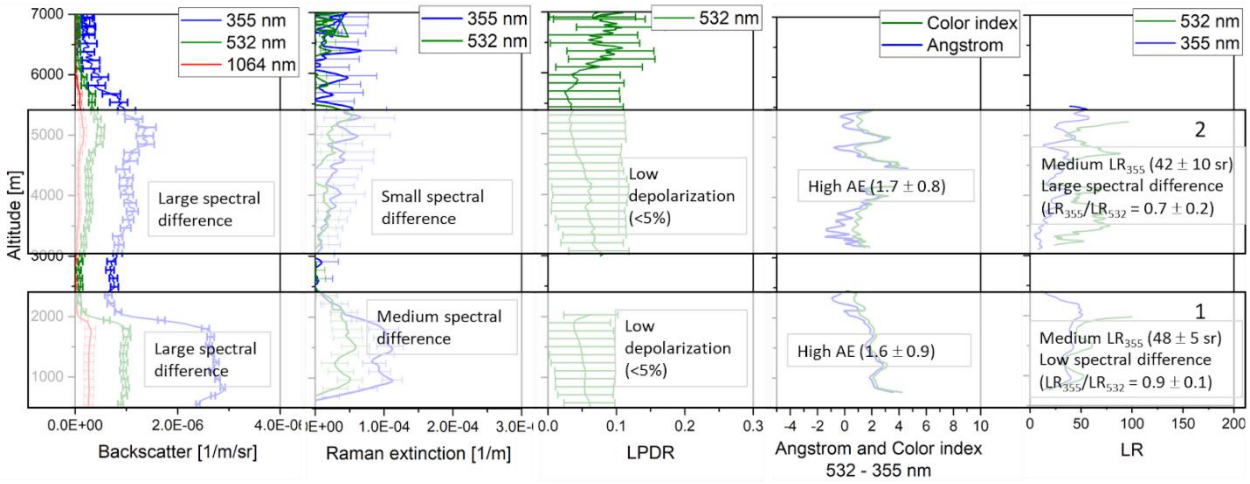

Figure 7 : *Profiles of aerosol optical properties at MARS on 19 March 2022, 17:49 – 21:41 UTC.*

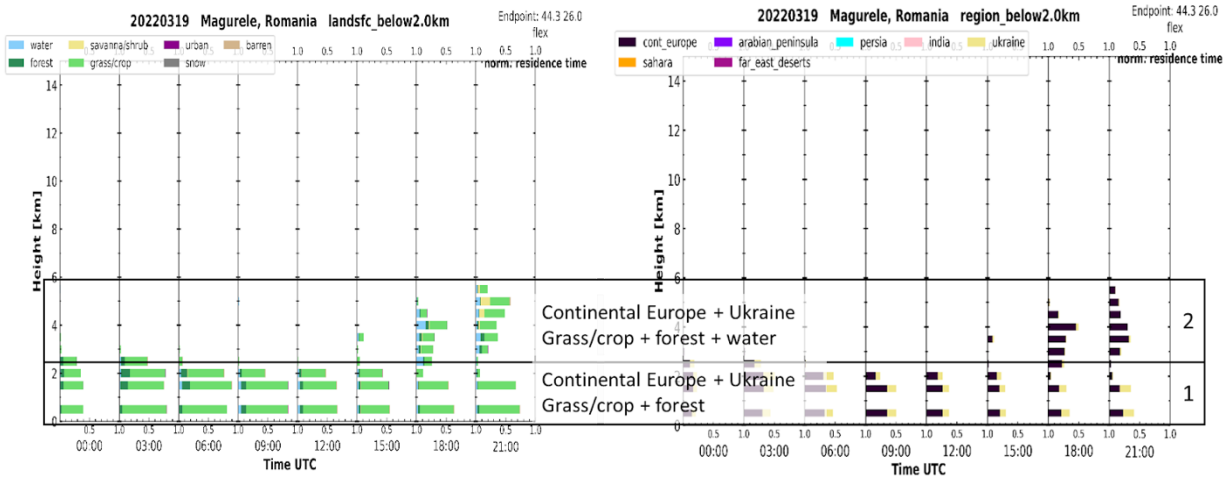

Figure 8 : *FLEXPART retrieval of the type (left panel) and sources (right panel) of aerosol particles arriving at various altitudes and times over MARS on 19 March 2022.*

RI-URBANS (www.RIURBANS.eu) is supported by the European Commission under the Horizon 2020 – Research and Innovation Framework Programme, H2020-GD-2020, Grant Agreement number: 101036245

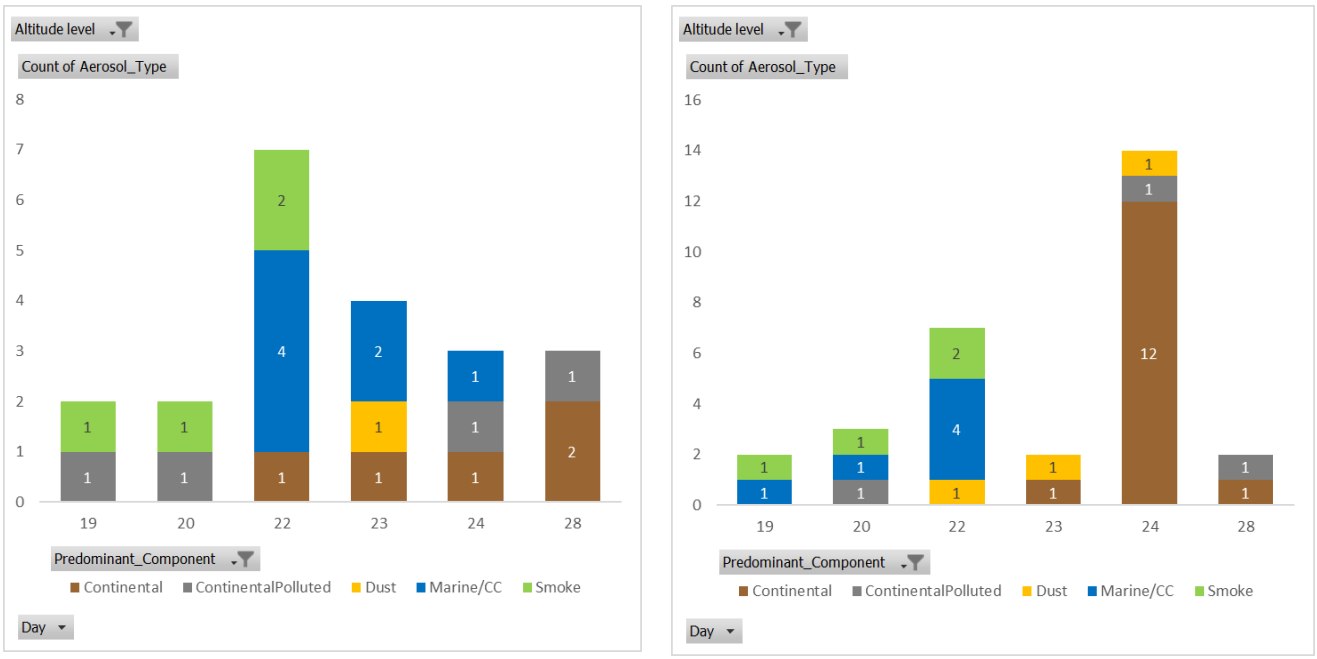

Figure 9 : *Daily NATALI retrievals of the aerosol type in the ABL (left panel, 0.5 - 2 km altitude) and free troposphere (right panel, > 2 km altitude) at MARS between 19 and 28 March 2022. The numbers inside the columns represent the number of layers of a certain type.*

3.3 Aerosol typing using depolarisation data from ALC - examples from Aosta, Rome and Paris

Following some first polarization-sensitive ALC prototypes (such as the one developed by Lufft in 2015 in the framework of the DIAPASON Project (Gobbi et al., 2019) that is since then operating in Rome), P-ALC with sufficient signal strength are now commercially available (e.g., VAISALA CL61) and are spreading in European ALC networks (e.g. E-PROFILE). Such systems are capable of measuring depolarisation profiles continuously, enabling the assessment of aerosol type and composition in synergy with other remote sensing/in-situ observations and models. For example, desert dust non-spherical particles are clearly detected during a strong Saharan dust intrusion in Italy in March 2022 (Figure 10), demonstrating the additional insights gained to support AQ monitoring applications. Both the system in Rome (prototype P-ALC) and the one (Vaisala CL61) in Aosta (North-West of Italy) nicely capture the dust layer characteristics in their depolarisation profiles, thereby considerably improving the capacity of ALC to distinguish aerosol types. In Rome, the polarization trace clearly shows that desert dust particles reach the lowest levels, i.e. impact local AQ, in the early hours of March 18.

RI-URBANS (www.RIURBANS.eu) is supported by the European Commission under the Horizon 2020 – Research and Innovation Framework Programme, H2020-GD-2020, Grant Agreement number: 101036245

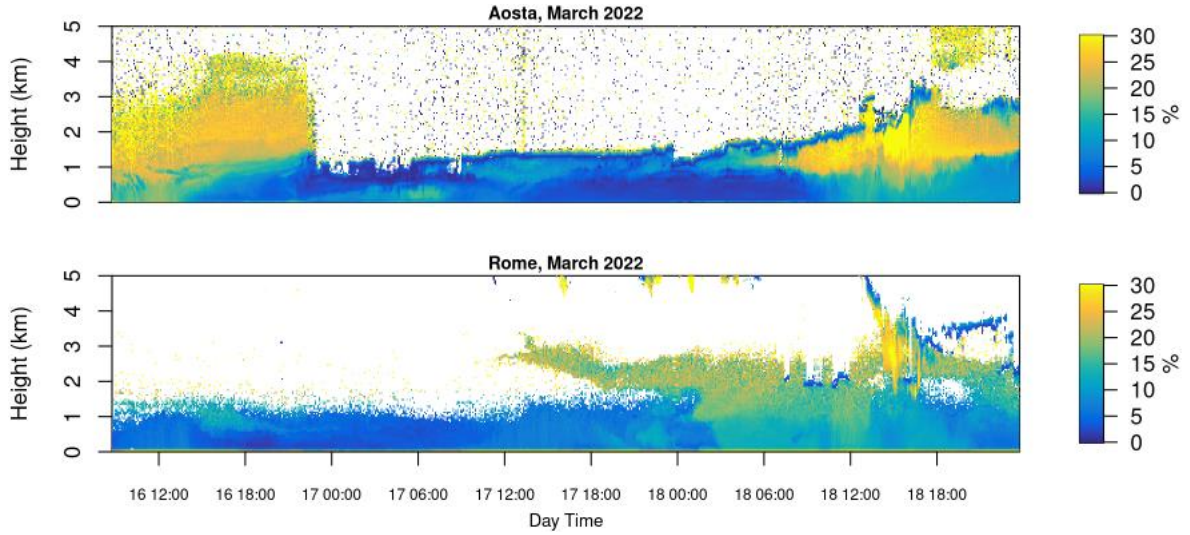

***Figure 10** : ALICEnet linear depolarization profiles in Aosta and Rome measured on16-18 March 2022 employing a CL-61 and the DIAPASON polarisation-sensitive P-CHM15K prototype, respectively.*

An example of dust-free conditions was observed by the P-ALC at Aosta on 5th April 2022 (Figure 11). On this day, locally-generated aerosols (e.g. soil-type particles resuspended by local convection) can be clearly seperated from those of regional origin (see phenomenon of Po Valley advection described in Section 3.4) as the latter are composed of non-depolarizing, spherical, hygroscopic particles. The parallel-polarization signal recorded by the P-ALC (Figure 11, top panel) shows a máximum aerosol load in the afternoon and early morning, which is explained by the regional transport mechanisms (Section 3.4). Conversely, by combining parallel and cross-polirized signals of the P-ALC, the derived depolarization information (Figure 11, bottom panel) reveals this regional haze to be composed of spherical particles and further identifies the local, non-spherical soil particles lofted by developing convection into the lowermost atmospheric levels in the middle of the day.

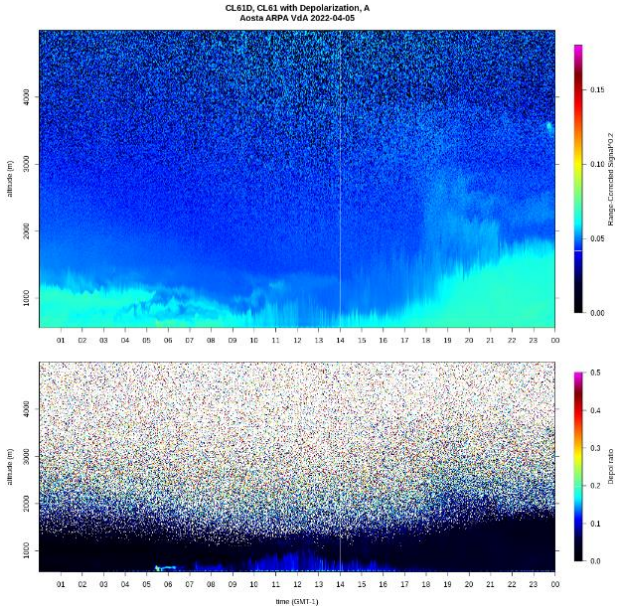

***Figure 11 :** ALICEnet aerosol signal (top) and linear depolarization (bottom) profiles as measured by P-ALC (Vaisala CL61) in Aosta on 5 April 2022*

RI-URBANS (www.RIURBANS.eu) is supported by the European Commission under the Horizon 2020 – Research and Innovation Framework Programme, H2020-GD-2020, Grant Agreement number: 101036245

A Vaisala CL61 P-ALC has been also operated in the Paris city centre since June 2022. Between 16-18 June 2022, a significant heat wave situation occurred with near +40°C peak temperatures due to a strong southerly flow that brought hot air and dust above the city originating from North Africa. Figure 12 shows the CL61 volume linear depolarization profile time series (0-0.3 in color scale) during the event as well as MLH derived using STRATfinder (Section 2.1). A dust layer is present at around 3000 m altitude on 16th June, subsiding significantly on the 17th June, when the MLH remained relatively shallow compared to typical June values. On the afternoon of 18 June, the mixing layer developed very rapidly due to a change in air mass aloft, destabilising the atmosphere and creating very strong vertical mixing. Dust aerosols were mixed all the way to the ground creating peak PM2.5 concentrations observed at the AQMN surface stations in Paris in the evening.

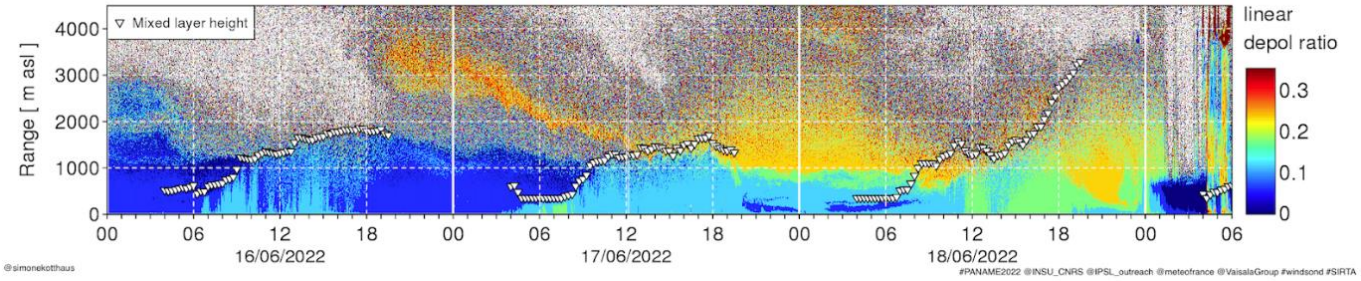

Figure 12 : *Vertical profiles of volume linear depolarization ratio retrieved from a Vaisala CL61 ALC operated in the Paris city centre by the SIRTA observatory. Mixing layer height values are retrieved from STRATfinder (see Section 2.1**).***

3.4 Aerosol regional transport impact on AQ: examples of the Po Valley

The operational use of active remote sensing from ALC systems has been a key tool to reveal and quantify the export of pollutants from the Po Valley to surrounding areas. A recent study performed using data collected in the northwestern Italian Alps showed that, mostly due to thermal winds producing typical mountain-valley daily circulations, Po Valley pollution markedly affects PM-related AQ in the surrounding 'pristine' mountain environments, namely the Alpine and pre-Alpine areas (Diemoz et al., 2019a, b). The phenomenon was first observed by lidar observations performed at the EC-JRC in Ispra (VA), about 60 km northwest of the Milan metropolitan area (Barnaba et al., 2010), and has been recently thoroughly investigated by means of continuous (24/7) data from the ALICEnet ALC systems at Milan and Aosta, respectively within and at the NW border of the Po Valley (Figure 13).

Figure 13: *Locations of the two ALICEnet ALC systems at Aosta and Milan in the Po Valley, Italy.*

Since 2015, the local EPA (Arpa Valle d'Aosta) is operating an ALC at Aosta to complement standard AQMN measurements. From the very beginning of its deployment, this system captured recurrent aerosol layers arriving in the afternoon and persisting during the night, characterising the aerosol vertical profiles up to 4 km altitude. It

RI-URBANS (www.RIURBANS.eu) is supported by the European Commission under the Horizon 2020 – Research and Innovation Framework Programme, H2020-GD-2020, Grant Agreement number: 101036245

has been demonstrated (Diemoz et al., 2019a, b) that this is a regional phenomenon mostly driven by mountain-valley breezes bringing polluted aerosol plumes from the Po Valley to the surrounding mountainous regions (Aosta, Figure 14a). Simultaneous ALC observations performed at the Po Valley pollution hotspot of Milan show how this phenomenon produces the reverse effect in the centre of the valley, i.e., a removal or 'cleaning' of PM in the afternoon hours (Figure 14b).

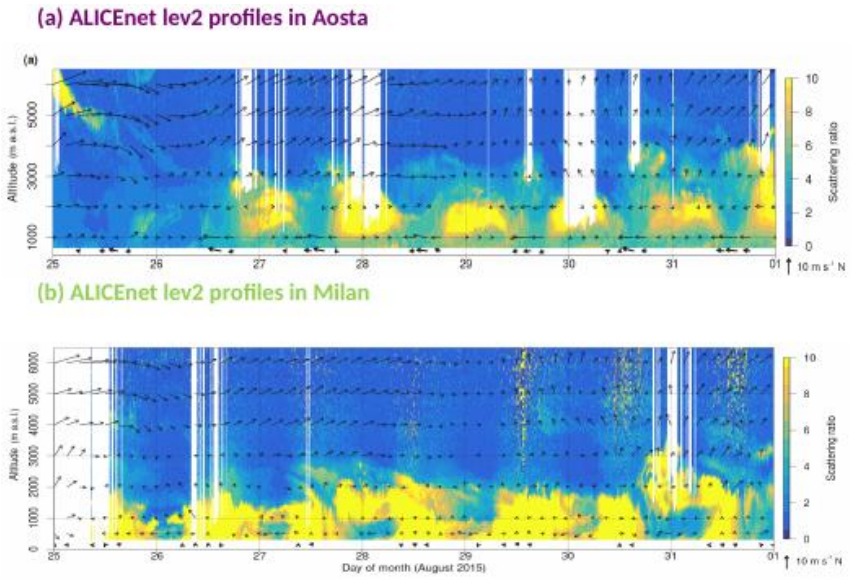

Figure 14 : *Continuous aerosol profiles (aerosol scattering ratio, ALICEnet Level 2 profiles) from ALC at Aosta and Milan in the period 25-31 August 2015. Adapted from Diemoz et al. 2019a.*

Overall, the operational use of ALC systems with support of modelling tools and in-situ AQMN observations revealed a major impact of such a regular, 'aerosol tide' on the trans-regional AQ. Based on 3 years of continuous measurements it was shown that in relatively 'clean' environments such as the Aosta Alpine area, this regular import from the Po Valley leads to a significant increase of PM_{10} concentrations (up-to a factor of 3.5). These aerosol-rich layers can extend to a depth of up to 4 km and are observed with a frequency of 50% of the days overall, which becomes 93% when only days with easterly winds (i.e., outflow from the Po Basin) are considered and 100% if air mass residence time over the Po Valley is > 10 h (Figure 15).

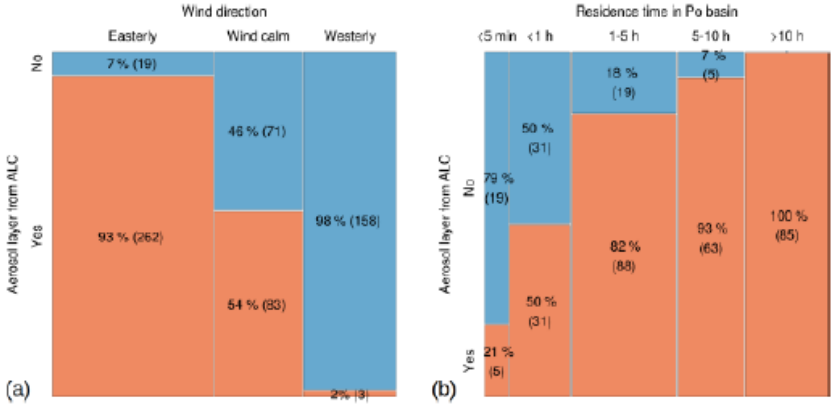

Figure 15 : *Contingency table based on 3-years (2015-2017) of continuous data showing occurrences of detection of the aerosol layer by the ALC in relation to a) wind direction and b) residence time of air masses in the Po Valley (evaluated by 48 h back-trajectories). The orange (blue) boxes represent cases when the aerosol layer is (is not) observed. Adapted from Diemoz et al. 2019b.*

RI-URBANS (www.RIURBANS.eu) is supported by the European Commission under the Horizon 2020 – Research and Innovation Framework Programme, H2020-GD-2020, Grant Agreement number: 101036245

Coupling of ALC observations with Positive Matrix Factorisation (PMF) of PM chemical properties at surface level revealed that particles advected from the Po Valley to the northwestern Alps are mostly of secondary origin and mainly composed of nitrates, sulphates, and ammonium. An important organic component was also detected in the warm season (Diemoz et al., 2019b).

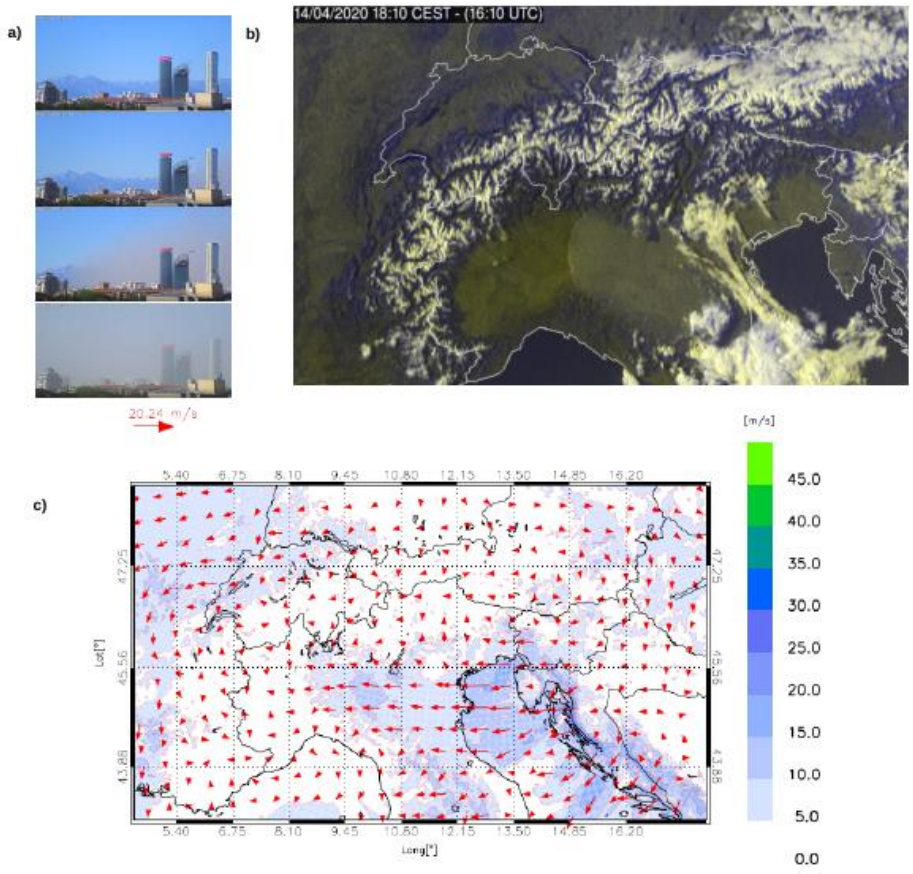

Figure 16*: a) Central Milan camera showing the rapid decrease of visibility/increase of PM on 14/07/2020 (from top to bottom: pictures at 16:08, 16:15, 16:20, 16:25 UTC), b) Po Valley satellite true color image, and c) 10 m wind speed and direction simulated by WRF over North Italy (14/07/2020 17:00 UTC, courtesy of Stefano Federico CNR/ISAC) illustrating the extension of the gust and wind fronts generating this effect.*

The operational deployment of ALC remote sensing systems also allows better understanding and interpretation of particular long and short range transport phenomena impacting PM-related AQ, including (but not limited to) desert dust or fire plumes. An example of this capability is provided below (Figure 16): a particular case of rapid and intense deterioration of PM AQ in the urban area of Milan in April 2020. The episode was due to an extended (about 100 km) gust front originating from the cold and intense Bora wind from East (Figure 16), raising and transporting farming residuals across the entire Po Valley. In fact, the episode was preceded by a particularly dry period, an anomalous condition affecting most of Europe in that month. Note that a quite similar event was recorded at the same sites also in April 2022.

The corresponding aerosol mass concentration profiles derived from ALC observations at Milan (Figure 17a) nicely capture the timing of the plume arrival and show the vertical extent of the particle-rich layer associated with the episode. The plume continued to travel westward and was detected by the ALC at Aosta (Figure 17b) four hours later, indicating a horizontal wind speed of more than 12 m/s.

RI-URBANS (www.RIURBANS.eu) is supported by the European Commission under the Horizon 2020 – Research and Innovation Framework Programme, H2020-GD-2020, Grant Agreement number: 101036245

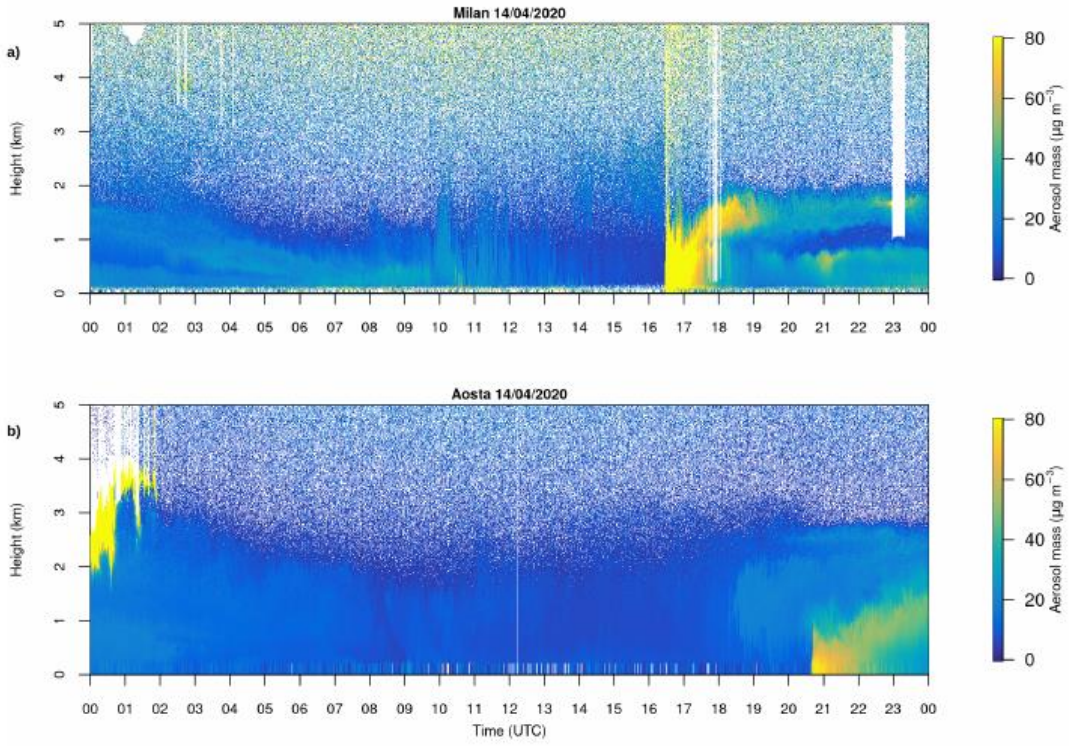

Figure 17: *ALICEnet aerosol mass profiles in a) Milan and b) Aosta, 14 April 2020.*

3.5 IAGOS in-situ profiling

The IAGOS in-situ profiles provide additional information about the lower troposphere, which are not available from surface stations or remote sensing instrumentation. They allow for the detection of layers of enhanced mixing ratios that were advected from remote source regions and can affect the urban air quality due to downmixing, and provide information about e.g., the vertical profile of the NO to NO2 ratio (Figure 18). The latter being difficult to retrieve from remote sensing measurements.

The comparison of IAGOS in-situ CO and O3 profiles close to the surface with ground stations at Frankfurt (Main) airport shows no strong impact by local emissions related to airport activities (red rhombus symbol). Petetin et al. (2018) showed furthermore that these observations have characteristics (mixing ratio distribution, seasonal variations, and trends) similar to the mixing ratios measured at surrounding urban background stations (Figure 19, blue cross).

Above the ABL, the correlation between the IAGOS in-situ and the urban background observations decreases rapidly while increasingly high correlations with remote Global Atmosphere Watch (GAW) stations like the Jungfraujoch observatory can be found (Figure 20).

RI-URBANS (www.RIURBANS.eu) is supported by the European Commission under the Horizon 2020 – Research and Innovation Framework Programme, H2020-GD-2020, Grant Agreement number: 101036245

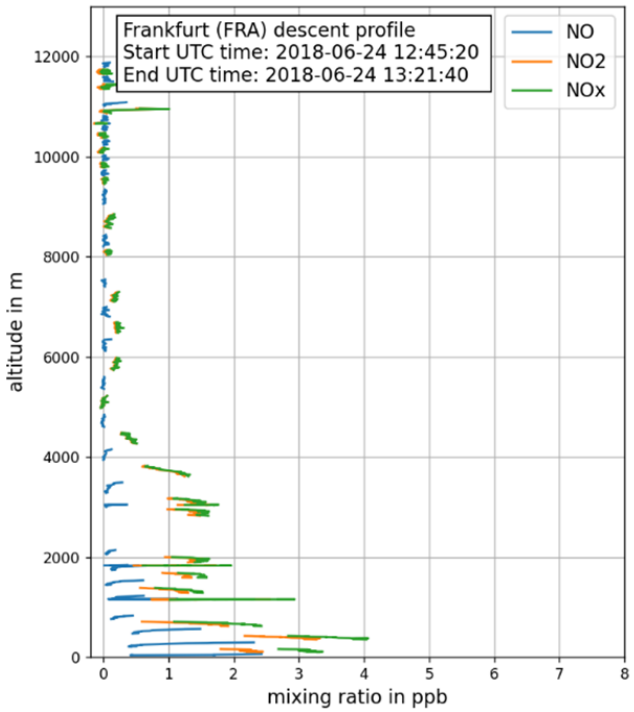

Figure 18: *IAGOS NO, NO_2, and NOx profiles over Frankfurt (Main) in 2018.*

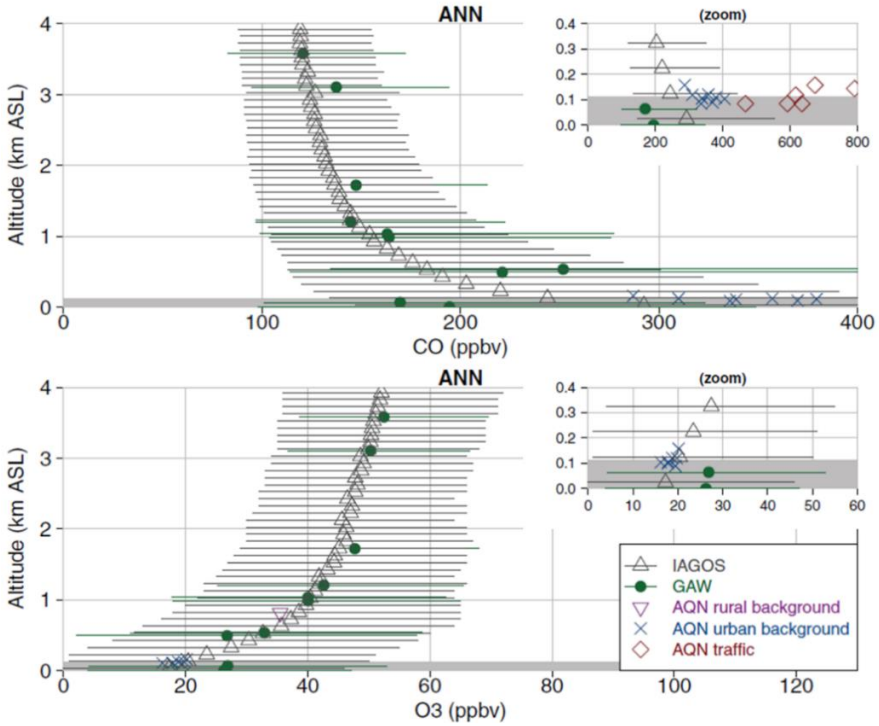

Figure 19: *IAGOS CO and O3 profiles compared with surface stations (Frankfurt 2002 -2012). Source: Fig. 5 from Petetin et al. (2018).*

RI-URBANS (www.RIURBANS.eu) is supported by the European Commission under the Horizon 2020 – Research and Innovation Framework Programme, H2020-GD-2020, Grant Agreement number: 101036245

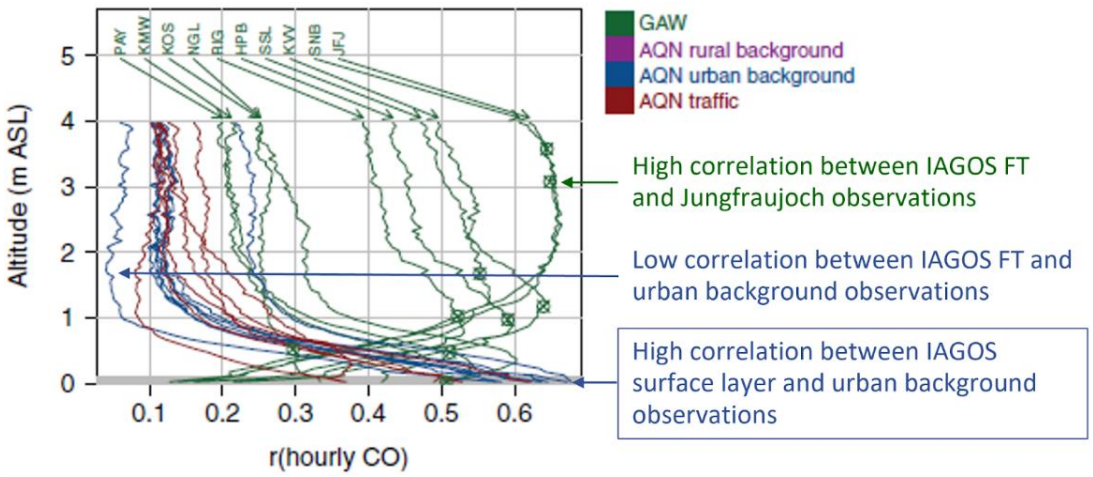

Figure 20 : *Correlation (r) profiles for IAGOS CO observations over Frankfurt (Main) airport (2002 -2012) with observations at surface stations. Source: Adapted from Fig. 7 in Petetin et al. (2018).*

3.6 Wind profiles

To capture both vertical profiles of horizontal wind and high-frequency fluctuations of vertical velocity, the Doppler wind lidar operational setup should include both DBS or VAD and vertical stare mode. Examples from the observations with a scanning Doppler wind lidar (Vaisala windcube WLS400) operated in central Paris, illustrate that average ABL flow patterns and its interaction with the free atmosphere (including e.g. wind shear) can be monitored continuously. The vertical velocity variance illustrates variations in atmospheric turbulence which can be critical in the context of AQ, as it affects e.g. mixing and entrainment velocities or the vertical dilution of atmospheric pollutants emitted at the surface.

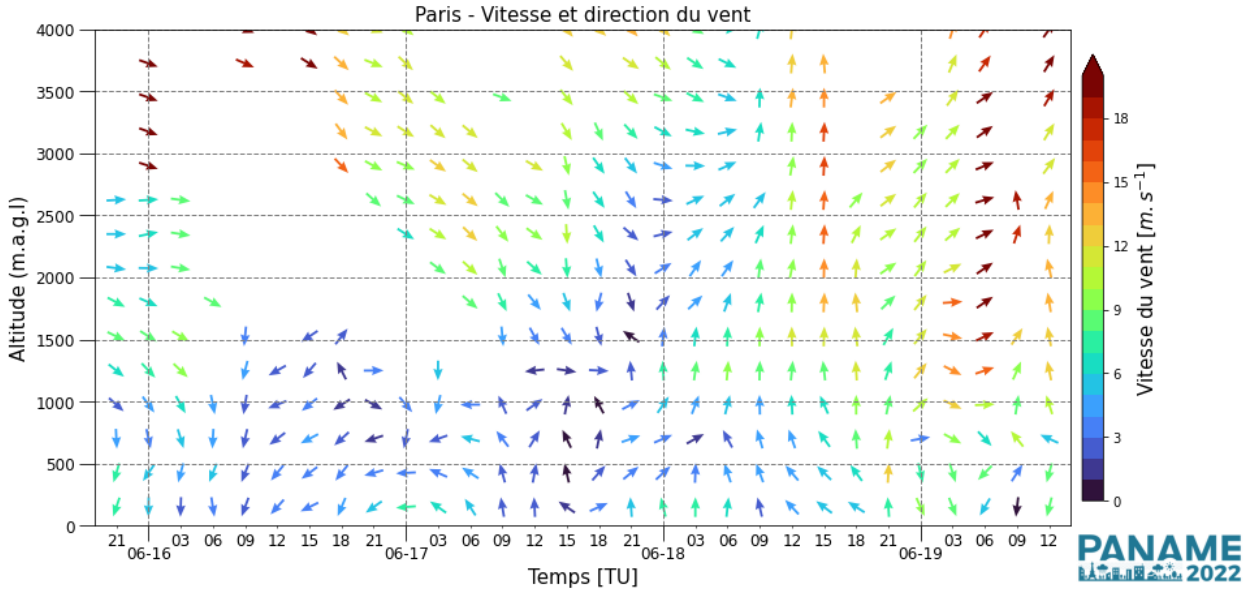

Figure 21 : Vertical profiles of horizontal wind (orientation of arrows indicates wind direction, colour indicates wind speed) observed with a VAISALA windcube WLS400 Doppler wind lidar using DBS at a central urban location in Paris (QUALAIR site at Sorbonne Université) during a heat event in June 2022.

On 17 June 2022 strong wind shear occured between a southerly flow in the boundary layer and a northerly flow aloft (Figure 21), while the southerly flow extends from the surface to 3000 m on the following day (18 June 2022). The diurnal cycle of the vertical velocity variance profile (Figure 22) clearly illustrates the diurnal evolution of the

RI-URBANS (www.RIURBANS.eu) is supported by the European Commission under the Horizon 2020 – Research and Innovation Framework Programme, H2020-GD-2020, Grant Agreement number: 101036245

mixed layer during daytime. Note that although limited to very shallow layers, vertical velocity variance remains non-zero at night at times. On June 18 after 18 UTC, significant vertical velocity variance is observed aloft (between 1500 and 3500 m), which resulted from cooler air advection above the ABL that destabilised the atmosphere and inducing strong vertical mixing. Peak PM2.5 concentrations were observed at the surface during that time as long-range transported dust aerosols were mixed downwards follwoing their entrainment into the ABL.

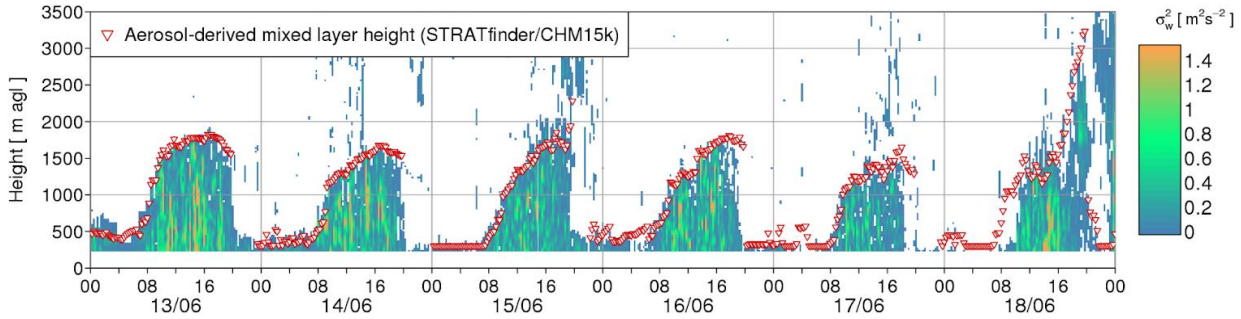

Figure 22 : *Vertical profiles of the variance of the vertical velocity observed in June 2022 in central Paris using a Vaisala windcube 400s in vertical stare mode with aerosol-derived mixed layer height (see Section 3.1).*

4 Measurement requirements

In this section instruments currently used in diverse networks (e.g. ACTRIS, IAGOS, E-PROFILE) are presented. Deriving high quality products from these instruments requires that they are operated following standard operating procedures and calibrated according to network standards. Four types of instruments are presented.

4.1 Automatic lidars and ceilometers (ALC)

ALC are compact, simple lidars that operate at wavelengths mostly in the infrared or visible spectral regions. Main output is the cloud base altitude and the profile of attenuated backscatter signal. The signal-to-noise ratio capabilities vary greatly between ALC due to the wide range of models available from various manufacturers. For aerosol-related studies, included the use of aerosol as tracer for ABLH/MLH retrievals, ALC performance may be limited in pristine environments where aerosol load is low or at elevated heights above the sensor (e.g., deep ABL development). Further details on ALC operations are summarised in Kotthaus et al. (2022). This review paper lists the following ALC capabilities which make them particularly useful for monitoring the atmospheric boundary layer:

- ALC can be operated continuously and autonomously under all weather conditions with very low maintenance so that their data have a much greater temporal coverage than those collected by high-power research-grade lidars that tend to focus on specific periods of interest.
- ALC have a smaller region of incomplete optical overlap compared to high-power lidar systems. This means they can provide quality observations even at very low altitudes above the surface which makes them more suitable for the characterisation of shallow layer.
- ALC are deployed at many locations, hence providing an unprecedented spatial coverage. Most airports are operating ALC for the purpose of monitoring the cloud base altitude. Where airports are located within or near cities, this can be a useful source of information.

RI-URBANS is implementing two automatic layer detection algorithms (Section 2.1) to account for a variety of ALC models with different signal strengths:

RI-URBANS (www.RIURBANS.eu) is supported by the European Commission under the Horizon 2020 – Research and Innovation Framework Programme, H2020-GD-2020, Grant Agreement number: 101036245

- STRATfinder is used for ALC with relatively high signal strength. Layer detection for the following models is:
  - operational: Lufft CHM15k
  - under development: Vaisala CL61, Cimel CE376
- CABAM is used for ALC with relatively low signal strength. Layer detection is operational for the Vaisala CL31, CL51.

ALC-based retrieval of aerosol properties profiles at different levels of accuracy is a current, in- progress activity within the scientific community, as demonstrated for example by the efforts done in this direction within the ongoing EU COST Action PROBE (https://www.probe-cost.eu). For the AQ community, aerosol mass concentration profiles are certainly among the most interesting products expected from these systems, as this metric is currently the only one regulated by the EU AQ Directive and thus routinely measured and modelled by regional and national AQ agencies. Still, the primary aerosol property derivable by ALC system is an optical one (namely, the aerosol backscatter) and some further assumptions are necessary to estimate aerosol volume, and thus mass, from it.

The following instrumental requirements are identified to derive advanced products (Section 2) from ALC observations:

- Operated automatically, autonomous, with remote control posible.
- Full overlap of the instrument laser beam and field-of-view within 300-500 m and suitable (instrument-specific) overlap correction procedures below this height.
- Sufficient signal-to-noise ratio up to at least 7-8 km for the detection and characterization of most long-range transported tropospheric aerosols layers and still able to reach 'aerosol-free' windows for Rayleigh-based calibration.
- Sufficiently high vertical and temporal resolution of raw data (around 15 m, 15 s) to follow rapid dynamics of both aerosol and cloud layers to be detected.
- Use of eye-safe emitted light in the UV-NIR range, out of major atmospheric gases absorption bands to avoid need of further corrections.

The listed instrumental requirements would allow retrieval of the attenuated aerosol backscatter profiles with adequate accuracy (Level 0 data). Still, estimation of PM profiles from these profiles further requires assumptions on the link between aerosol backscatter and other aerosol properties including aerosol mass. In fact, this link can be site and/or aerosol type specific, so that PM retrievals based on ALC data requires further development of specific algorithms.

In this document, the ALC-based PM retrievals cases shown (e.g. Figure 2 and Figure 14), were obtained using the algortitm described in Dionisi et al., (2018) and currently implemented and tested within the italian ALC network ALICEnet.

4.2 High-Power Aerosol Lidars

High-power aerosol lidars are often located and operated at suburban or rural sites. They are useful to characterise background conditions. These instruments are typically high-power, multi-wavelength (backscatter at 1064, 532 and 355 nm, extinction at 532 and 355 nm) systems that are typically operated at night for selected cases. When complemented with multi-wavelength photometers concentration profiles can be derived.

The following requirements need to be fulfilled to retrieve the products presented in Section 2:

- Overlap below 300m (**optical profiles**) for allowing low altitude investigation.
- Minimum high altitude > 15 km (**range corrected signals**) for allowing detection and characterization of the long-range transported aerosols in the troposphere and lower stratosphere.

RI-URBANS (www.RIURBANS.eu) is supported by the European Commission under the Horizon 2020 – Research and Innovation Framework Programme, H2020-GD-2020, Grant Agreement number: 101036245

- Height resolution raw <15 m (recorded signal) for allowing layer and cloud discrimination.
- Time resolution raw < 60 s (recorded signal) for allowing cloud screening.
- Multiwavelength profiles (**aerosol typing** and **concentration profiles**).
- Depolarization profile at least at 1 wavelength (**aerosol typing** and **concentration profiles**).
- Co-located photometer being part of AERONET (**microphysical properties** and **concentration profiles**).
- ACTRIS/EARLINET format (**optical profiles**, **aerosol typing**).
- Use of a standard retrieval algorithm called Single Calculus Chain (**all the products**).

4.3 In-situ profiling

The IAGOS-CORE instrumentation is dedicated to measure the key climate variables in the atmosphere (troposphere and UTLS region). It consists of Package 1 (P1) which is installed on all IAGOS-CORE aircraft and Package 2 (P2) where optionally 4 different types of instruments can be installed. All instruments are designed for autonomous operation over periods of up to 6 months. The actual deployment on an aircraft can be shorter if, e.g., contamination or loss of sensitivity is encountered. All instruments switch between standby (on ground) and normal operation mode (in air) using the signals of aircraft speed and/or the weight on wheel signal of the aircraft. The data are transmitted on ground using "the cargo door opened" signal via telecommunication (GSM) to the IAGOS data centre.

For the main European carriers Lufthansa and Air France, the IAGOS profile measurements in Europe are mainly available at the hubs Frankfurt (Lufthansa) and Paris (Air France).

P1 is the basic instrument of IAGOS. It is designed for the autonomous measurement of ozone and carbon monoxide and contains the data acquisition for the IAGOS relative Humidity Sensor (ICH) and the Backscatter Cloud Probe (BCP). It also records the position of the aircraft and provides data transmission for all IAGOS instruments connected with P1 via GSM.

Ozone (O_3) is measured by UV absorption at 253.7 nm, using the optical block of a Thermo Instruments Model 49 analyser. Ozone free air is generated by passing the ambient air through a scrubber. In flight calibration checks are made with a built-in ozone generator.

Time resolution: 4s
Precision: ±2%
Accuracy: ±2 ppb

Carbon monoxide (CO) is measured by infrared absorption using the gas filter correlation technique. In order to achieve larger sensitivity and time response, the absorption cell is operated at 2 bar and at a flow rate of 4 SLM. The IR detectors are peltier cooled for noise reduction. In-flight calibration includes regular measurements of CO-free air generated by passing the dried ambient air over a bed of Sofnocat.

Time resolution: 30s
Precision: ±5%
Accuracy: ±5 ppb

A more detailed technical overview of the IAGOS-CORE ozone and carbon monoxide measurements is given by Nédélec et al. (2015).

RI-URBANS (www.RIURBANS.eu) is supported by the European Commission under the Horizon 2020 – Research and Innovation Framework Programme, H2020-GD-2020, Grant Agreement number: 101036245

The P2b instrument is designed for the autonomous measurement of **nitrogen oxides (NO_X)**. NO_x is defined as the **sum of nitrogen monoxide (NO) and nitrogen dioxide (NO_2)**. The measurement principle is based on chemiluminescence, i.e., the photoelectric detection of the light (hv) produced in a chemical reaction (R1) between atmospheric NO and ozone (O_3). Conversion of NO_2 to NO is achieved by photolytic conversion (R2) using the light of 4 UV-LEDs.

R1: $NO + O_3 \Rightarrow NO_2 + O_2 + hv \quad (600 < \lambda < 3000\ nm)$

R2: $NO_2 + hv + O_2 \Rightarrow NO + O_3 \quad (\lambda = 390\ nm)$

The instrument measures NO and NO_x sequentially, by switching the LEDs of the converter off and on.

The P2b instrumentation consists of the instrument unit and two pressure cylinders, which provide oxygen and synthetic air for operation and in-flight calibration. The instrument is connected with PFA tubing to the inlet (Rosemount TAT housing) at the fuselage. P2b is connected with P1 via Ethernet for data transmission.

Time resolution:	4s (not all intervals contain data; sequential measurement of NO and NO_x)
Precision:	NO: ±5% or ±25 ppt (4s, 1 sigma); NO_x: ±5% or ±35 ppt (4s, 1 sigma)
Accuracy:	NO: ±7% or ±25 ppt (1 sigma); NO_x: ±15% or ±40 ppt (1 sigma)
Interferences:	HONO (8%); potentially HNO_4 and PAN

Further details on the characterisation of the P2b NO_x instrument are described by Berkes et al. (2018).

The upcoming air quality instrument (P2e) is designed for the autonomous measurement of nitrogen dioxide (NO_2; limit of detection as low as 0.1 ppbv) and aerosol light extinction (at 450 nm and 630 nm) using the cavity attenuated phase shift method (CAPS). It measures the total particle number concentration by means of a water condensation particle counter (MAGIC CPC (Aerosol Devices) and the aerosol particle size distribution (diameter range: 125 nm to 3.5 µm) using a modified Portable Optical Particle Spectrometer (POPS, NOAA, FZJ). P2e has passed all qualification tests. It is expected to receive the Supplemental Type Certificate (STC) at the end of October 2022 by the European Union Aviation Safety Agency (EASA) which is needed for worldwide aircraft operation.

The standard operating procedure (SOP) documents are made available by the IAGOS research infrastructure (see documents linked on the following websites: For CO and O_3 (P1): https://www.iagos.org/iagos-core-instruments/package1/ ; for NO_x (P2b): https://www.iagos.org/iagos-core-instruments/package2b/; for P2e the SOP will be made available after certification).

4.4 Doppler and wind lidars

Doppler wind Lidars (DL) are active remote sensing systems similar to aerosol backscatter lidars. Heterodyne DL are mostly used to probe the atmospheric boundary layer; they operate at wavelengths between 1.5-2.0 µm. Based on the detected Doppler shift between the emitted and backscattered radiation, the radial velocity along the laser beam direction can be derived. By combining beams in multiple directions, the three wind components can be retrieved along a vertical profile. Using high temporal resolution data, indicators of atmospheric turbulence, such as the vertical velocity variance or the eddy dissipation rate can be calculated as advanced products. Further details on DL capabilities and limitations are summarised in Kotthaus et al. (2022).

To derive vertical profiles of horizontal wind and indicators of turbulence, RI-URBANS is recommending to include both DBS (or VAD) scans as well as vertical stare for at least 2-5 consecutive minutes at high temporal resolution into the Lidar operational setup. A vertical resolution of commonly 25-75 m is recommended.

RI-URBANS (www.RIURBANS.eu) is supported by the European Commission under the Horizon 2020 – Research and Innovation Framework Programme, H2020-GD-2020, Grant Agreement number: 101036245

A standard operating procedure document is made available by the Centre for Cloud Remote Sensing of the ACTRIS research infrastructure (see document on the following website: https://www.actris.eu/topical-centre/ccres/doppler-lidar).

5 References

Barnaba F, Putaud J, Gruening C, Dell`Acqua A, Martins Dos Santos S. (2010). Annual cycle in co-located in situ, total-column, and height resolved aerosol observations in the Po Valley (Italy): Implications for ground-level particulate matter mass concentration estimation from remote sensing. *Journal of Geophysical Research-Atmosphere*, 115, D19209.

Bellini, A., Diémoz, H., Di Liberto, L., Gobbi, G.P., Barnaba, F.: Monitoring the aerosol vertical profiles across Italy with Alicenet: retrievals and applications for air quality and multi risk-warning systems, to be submitted to AMT 2022. See https://www.alice-net.eu/documents/AlicenetEGU22.pdf

Berkes, F., Houben, N., Bundke, U., Franke, H., Pätz, H. W., Rohrer, F., ... & Petzold, A. (2018). The IAGOS NO x instrument–design, operation and first results from deployment aboard passenger aircraft. *Atmospheric measurement techniques*, *11*(6), 3737-3757.

Chaikovsky, A., Dubovik, O., Holben, B., Bril, A., Goloub, P., Tanré, D., Pappalardo, G., Wandinger, U., Chaikovskaya, L., Denisov, S., Grudo, J., Lopatin, A., Karol, Y., Lapyonok, T., Amiridis, V., Ansmann, A., Apituley, A., Allados-Arboledas, L., Binietoglou, I., Boselli, A., D'Amico, G., Freudenthaler, V., Giles, D., Granados-Muñoz, M. J., Kokkalis, P., Nicolae, D., Oshchepkov, S., Papayannis, A., Perrone, M. R., Pietruczuk, A., Rocadenbosch, F., Sicard, M., Slutsker, I., Talianu, C., De Tomasi, F., Tsekeri, A., Wagner, J., and Wang, X.: Lidar-Radiometer Inversion Code (LIRIC) for the retrieval of vertical aerosol properties from combined lidar/radiometer data: development and distribution in EARLINET, Atmos. Meas. Tech., 9, 1181–1205, https://doi.org/10.5194/amt-9-1181-2016, 2016.

D'Amico, G., Amodeo, A., Baars, H., Binietoglou, I., Freudenthaler, V., Mattis, I., ... & Pappalardo, G. (2015). EARLINET Single Calculus Chain–overview on methodology and strategy. *Atmospheric Measurement Techniques*, *8*(11), 4891-4916.

D'Amico, G., Amodeo, A., Mattis, I., Freudenthaler, V., and Pappalardo, G. : EARLINET Single Calculus Chain – technical – Part 1: Pre-processing of raw lidar data, Atmos. Meas. Tech., 9, 491-507, doi:10.5194/amt-9-491-2016, 2016.

Diémoz, H., Barnaba, F., Magri, T., Pession, G., Dionisi, D., Pittavino, S., ... & Gobbi, G. P. (2019a). Transport of Po Valley aerosol pollution to the northwestern Alps–Part 1: Phenomenology. *Atmospheric Chemistry and Physics*, *19*(5), 3065-3095.

Diémoz, H., Gobbi, G. P., Magri, T., Pession, G., Pittavino, S., Tombolato, I. K., ... & Barnaba, F. (2019b). Transport of Po Valley aerosol pollution to the northwestern Alps–Part 2: Long-term impact on air quality. *Atmospheric Chemistry and Physics*, *19*(15), 10129-10160.

Dionisi, D., Barnaba, F., Diémoz, H., Di Liberto, L., and Gobbi, G. P. (2018). A multiwavelength numerical model in support of quantitative retrievals of aerosol properties from automated lidar ceilometers and test applications for AOT and PM10 estimation, *Atmos. Meas. Tech.*, 11, 6013–6042, https://doi.org/10.5194/amt-11-6013-2018

Gobbi, G. P., Barnaba, F., Di Liberto, L., Bolignano, A., Lucarelli, F., Nava, S., ... & Wille, H. (2019). An inclusive view of Saharan dust advections to Italy and the Central Mediterranean. *Atmospheric environment*, *201*, 242-256.

RI-URBANS (www.RIURBANS.eu) is supported by the European Commission under the Horizon 2020 – Research and Innovation Framework Programme, H2020-GD-2020, Grant Agreement number: 101036245

Kebabian, P. L., Wood, E. C., Herndon, S. C., & Freedman, A. (2008). A practical alternative to chemiluminescence-based detection of nitrogen dioxide: Cavity attenuated phase shift spectroscopy. *Environmental science & technology*, *42*(16), 6040-6045.

Kotthaus, S., Haeffelin, M., Drouin, M. A., Dupont, J. C., Grimmond, S., Haefele, A., ... & Wiegner, M. (2020). Tailored algorithms for the detection of the atmospheric boundary layer height from common automatic lidars and ceilometers (Alc). *Remote Sensing*, *12*(19), 3259.

Kotthaus, S., Bravo-Aranda, J. A., Collaud Coen, M., Guerrero-Rascado, J. L., Costa, M. J., Cimini, D., ... & Haeffelin, M. (2022). Atmospheric boundary layer height from ground-based remote sensing: a review of capabilities and limitations. *Atmospheric Measurement Techniques Discussions*, 1-88.

Liu, Z., Barlow, J. F., Chan, P. W., Fung, J. C. H., Li, Y., Ren, C., ... & Ng, E. (2019). A review of progress and applications of pulsed Doppler wind LiDARs. *Remote Sensing*, *11*(21), 2522.

Lopatin, A., Dubovik, O., Chaikovsky, A., Goloub, P., Lapyonok, T., Tanré, D., & Litvinov, P. (2013). Enhancement of aerosol characterization using synergy of lidar and sun-photometer coincident observations: the GARRLiC algorithm. *Atmospheric Measurement Techniques*, *6*(8), 2065-2088.

Mattis, I., D'Amico, G., Baars, H., Amodeo, A., Madonna, F., and Iarlori, M., EARLINET Single Calculus Chain – technical Part 2: Calculation of optical products, Atmos. Meas. Tech., 9, 3009-3029, doi:10.5194/amt-9-3009-2016, 2016.

Mona, L., Amodeo, A., D'Amico, G., Giunta, A., Madonna, F., and Pappalardo, G.: Multi-wavelength Raman lidar observations of the Eyjafjallajökull volcanic cloud over Potenza, southern Italy, Atmos. Chem. Phys., 12, 2229–2244, https://doi.org/10.5194/acp-12-2229-2012, 2012.

Mona, L., D'Amico, G., Gagliardi, S., Amato, F., Amodeo, A., Ciamprone, S., De Rosa, B., Ripepi, E., Summa, D., Alados-Arboledas, L., Amiridis, V., Baars, H., Kompula, M., Mattis, I., Nicolae, D., Pietras, C., Stachlewska, I. S., and Peuch, V. H.: Pilot provision of EARLINET/ACTRIS lidar profiles to CAMS, EGU General Assembly 2021, online, 19–30 Apr 2021, EGU21-14943, https://doi.org/10.5194/egusphere-egu21-14943, 2021.

Müller, D., Chemyakin, E., Kolgotin, A., Ferrare, R. A., Hostetler, C. A., & Romanov, A. (2019). Automated, unsupervised inversion of multiwavelength lidar data with TiARA: assessment of retrieval performance of microphysical parameters using simulated data. *Applied optics*, *58*(18), 4981-5008.

Nédélec, P., Blot, R., Boulanger, D., Athier, G., Cousin, J. M., Gautron, B., ... & Thouret, V. (2015). Instrumentation on commercial aircraft for monitoring the atmospheric composition on a global scale: the IAGOS system, technical overview of ozone and carbon monoxide measurements. *Tellus B: Chemical and Physical Meteorology*, *67*(1), 27791.

Nicolae, D., Vasilescu, J., Talianu, C., Binietoglou, I., Nicolae, V., Andrei, S., and Antonescu, B.: A neural network aerosol-typing algorithm based on lidar data, Atmos. Chem. Phys., 18, 14511–14537, https://doi.org/10.5194/acp-18-14511-2018, 2018.

Papagiannopoulos, N., Mona, L., Amodeo, A., D'Amico, G., Gumà Claramunt, P., Pappalardo, G., Alados-Arboledas, L., Guerrero-Rascado, J. L., Amiridis, V., Kokkalis, P., Apituley, A., Baars, H., Schwarz, A., Wandinger, U., Binietoglou, I., Nicolae, D., Bortoli, D., Comerón, A., Rodríguez-Gómez, A., Sicard, M., Papayannis, A., and Wiegner, M.: An automatic observation-based aerosol typing method for EARLINET, Atmos. Chem. Phys., 18, 15879–15901, https://doi.org/10.5194/acp-18-15879-2018, 2018.

RI-URBANS (www.RIURBANS.eu) is supported by the European Commission under the Horizon 2020 – Research and Innovation Framework Programme, H2020-GD-2020, Grant Agreement number: 101036245

Pappalardo, G., Amodeo, A., Apituley, A., Comeron, A., Freudenthaler, V., Linné, H., Ansmann, A., Bösenberg, J., D'Amico, G., Mattis, I., Mona, L., Wandinger, U., Amiridis, V., Alados-Arboledas, L., Nicolae, D., and Wiegner, M., EARLINET: towards an advanced sustainable European aerosol lidar network, Atmos. Meas. Tech., 7, 2389–2409, www.atmos-meas-tech.net/7/2389/2014/, doi:10.5194/amt-7-2389-2014, (2014).

Petetin, H., Jeoffrion, M., Sauvage, B., Athier, G., Blot, R., Boulanger, D., ... & Thouret, V. (2018). Representativeness of the IAGOS airborne measurements in the lower troposphere. *Elementa: Science of the Anthropocene*, *6*: 23. DOI: https://doi.org/10.1525/elementa.280

Pisso, I., Sollum, E., Grythe, H., Kristiansen, N. I., Cassiani, M., Eckhardt, S., Arnold, D., Morton, D., Thompson, R. L., Groot Zwaaftink, C. D., Evangeliou, N., Sodemann, H., Haimberger, L., Henne, S., Brunner, D., Burkhart, J. F., Fouilloux, A., Brioude, J., Philipp, A., Seibert, P., and Stohl, A.: The Lagrangian particle dispersion model FLEXPART version 10.4, Geosci. Model Dev., 12, 4955–4997, https://doi.org/10.5194/gmd-12-4955-2019, 2019.

Stein, A.F., Draxler, R.R, Rolph, G.D., Stunder, B.J.B., Cohen, M.D., and Ngan, F., (2015). NOAA's HYSPLIT atmospheric transport and dispersion modeling system, Bull. Amer. Meteor. Soc., 96, 2059-2077, http://dx.doi.org/10.1175/BAMS-D-14-00110.1

Tsekeri, A., Lopatin, A., Amiridis, V., Marinou, E., Igloffstein, J., Siomos, N., Solomos, S., Kokkalis, P., Engelmann, R., Baars, H., Gratsea, M., Raptis, P. I., Binietoglou, I., Mihalopoulos, N., Kalivitis, N., Kouvarakis, G., Bartsotas, N., Kallos, G., Basart, S., Schuettemeyer, D., Wandinger, U., Ansmann, A., Chaikovsky, A. P., and Dubovik, O.: GARRLiC and LIRIC: strengths and limitations for the characterization of dust and marine particles along with their mixtures, Atmos. Meas. Tech., 10, 4995–5016, https://doi.org/10.5194/amt-10-4995-2017, 2017.

Veselovskii, I., Dubovik, O., Kolgotin, A., Korenskiy, M., Whiteman, D. N., Allakhverdiev, K., & Huseyinoglu, F. (2012). Linear estimation of particle bulk parameters from multi-wavelength lidar measurements. *Atmospheric Measurement Techniques*, *5*(5), 1135-1145.

Vivone, G., D'Amico, G., Summa, D., Lolli, S., Amodeo, A., Bortoli, D., and Pappalardo, G.: Atmospheric boundary layer height estimation from aerosol lidar: a new approach based on morphological image processing techniques, Atmos. Chem. Phys., 21, 4249–4265, https://doi.org/10.5194/acp-21-4249-2021, 2021.

Voudouri, K. A., Siomos, N., Michailidis, K., Papagiannopoulos, N., Mona, L., Cornacchia, C., Nicolae, D., and Balis, D.: Comparison of two automated aerosol typing methods and their application to an EARLINET station, Atmos. Chem. Phys., 19, 10961–10980, https://doi.org/10.5194/acp-19-10961-2019, 2019.

RI-URBANS (www.RIURBANS.eu) is supported by the European Commission under the Horizon 2020 – Research and Innovation Framework Programme, H2020-GD-2020, Grant Agreement number: 101036245